Structure and Infrastructure Engineering: Maintenance, Management, Life-Cycle Design and Performance

Publication details, including instructions for authors and subscription information:
http://www.tandfonline.com/loi/nsie20

Structural damage detection and localisation using multivariate regression models and two-sample control statistics

S. Golnaz Shahidi[a], Mallory B. Nigro[a], Shamim N. Pakzad[a] & Yuchen Pan[a]

[a] Civil and Environmental Engineering Department, Lehigh University, 117 ATLSS Drive, Bethlehem, PA 18015, USA

Published online: 19 Aug 2014.

To cite this article: S. Golnaz Shahidi, Mallory B. Nigro, Shamim N. Pakzad & Yuchen Pan (2014): Structural damage detection and localisation using multivariate regression models and two-sample control statistics, Structure and Infrastructure Engineering: Maintenance, Management, Life-Cycle Design and Performance, DOI: 10.1080/15732479.2014.949277

To link to this article: http://dx.doi.org/10.1080/15732479.2014.949277

Structure and Infrastructure Engineering, 2014
http://dx.doi.org/10.1080/15732479.2014.949277

Structural damage detection and localisation using multivariate regression models and two-sample control statistics

S. Golnaz Shahidi*, Mallory B. Nigro[1], Shamim N. Pakzad[2] and Yuchen Pan[3]

Civil and Environmental Engineering Department, Lehigh University, 117 ATLSS Drive, Bethlehem, PA 18015, USA

(*Received 10 December 2013; final version received 2 May 2014; accepted 31 May 2014*)

This paper presents model-free damage identification and localisation methods based on two-sample control statistics as well as damage-sensitive features to be extracted from single- and multivariate regression models. For this purpose, sequential normalised likelihood ratio test and two-sample *t*-test are adopted to detect the change in two families of damage features based on the coefficients of four different linear regression models. The performance of combinations of these damage features, regression models and control statistics are compared through a scaled two-bay steel frame instrumented with a dense sensor network and excited by impact loading. It is shown that the presented methodologies are successful in detecting the timing and location of the structural damage, while having acceptable false detection quality. In addition, it is observed that incorporating multiple mathematical models, damage-sensitive features and change detection tests improve the overall performance of these model-free vibration-based structural damage detection procedures.

Keywords: damage detection; structural health monitoring; statistical analysis; regression models

1. Introduction

Structural health monitoring (SHM) research is mainly concerned with developing methodologies to assess the condition of constructed structures which are inevitably prone to deterioration and damage with use and time. To this end, numerous vibration-based structural damage detection techniques have been proposed that can be classified based on the features they interpret as damage indicators and/or their approaches (physics based or data driven).

Modal parameters (vibration frequencies, mode shapes, mode shape curvatures, etc.) have been widely used as damage-sensitive features in the SHM field (Doebling, Farrar, & Prime, 1998; Pandey & Biswas, 1995; West, 1984). However, since these damage indicators are global in nature, they are generally unable to detect local damages. In addition, they require measurement data with high signal to noise ratio as well as moderate damage levels to identify the damage in the system (Alvandi & Cremona, 2006; Farrar et al., 1994). As the identification of the structural damage in its early stages is essential in minimising the maintenance cost of the existing structures, research is still ongoing to extract features from structural responses that are sensitive enough to local and minor damage, yet robust to the common changes in the structural responses and measurement noise. Examples of such damage indicators are statistical features generated from sensor networks data (Dorvash et al., 2010; Figueiredo, Figueiras, Park, Farrar, & Worden, 2011; Kiremidjian, Kiremidjian, & Sarabandi, 2011; Nair, Kiremidjian, & Law, 2006; Yao & Pakzad, 2013). Such features seem more promising for applications on in-service structures, as with the recent advancement in sensing technology, literature reports numerous successful implementations of sensor networks on large-scale structures (e.g. Cruz & Salgado, 2009; Hu, Wang, & Ji, 2013; Jang, Spencer, Rice, & Wang, 2011; Labuz, Pakzad, & Wurst, 2011; Lynch, Wang, Loh, Yi, & Yun, 2006; Pakzad, 2010).

Damage identification methods can also be categorised into model-based and model-free approaches. In model-based damage detection procedures, certain parameters of a finite element simulation of the system are updated with respect to the measured responses to identify the existence and extent of the structural damage (Jaishi & Ren, 2006; Kim & Kawatani, 2008; Moaveni, Stavridis, Lombaert, Conte, & Shing, 2013; Weber & Paultre, 2010). While these methods are more objective in the interpretation of their results, their efficiency and performance depend on a priori knowledge of the material properties, boundary conditions and the location of the damage. On the other hand, model-free approaches use the measured responses directly in numerical algorithms so that there is no need for prior information about the structure's properties or suspected location of damage (Bodeux & Golinval, 2003; Deraemaeker & Preumont, 2006; Kumar, Oshima,

*Corresponding author. Email: sgs310@lehigh.edu

Mikami, Miyamori, & Yamazaki, 2012; Lu & Gao, 2005). These data-driven approaches are less laborious to implement and still effective in reflecting the changes in the structure's behaviour; however, they are dependent on statistical analysis to determine the significance of the changes in the monitoring data, distinguishing between assignable and common changes, a distinction that is extremely vital in structural damage detection.

This study presents model-free damage identification and localisation methods based on two-sample control statistics. The contribution of this paper is in establishing and comparing the effectiveness of different regression models, damage indicators and two-sample test methodologies for SHM applications. In addition, a damage-sensitive feature based on the change in the angle of regression coefficient vectors is introduced which is applicable to both single-variate regression (SVR) and multivariate regression models. The application of the collinear regression (CR) model and sequential two-sample statistical tests for damage detection and localisation is also introduced in this paper for the first time.

The comparison is made on the performance of combinations of damage features, regression models and control statistics on a scaled two-bay steel frame instrumented with a localised sensor array. The acceleration response of the frame recorded from two different physical states and the control charts are used to find the significance of change between the two. The first state is a baseline healthy state of the structure, and the second is an unknown state. In effect, two sets of data are created that would be taken from a structure pre- and post-damaging event (or a regular maintenance check). Linear regression parameters are generated to be utilised in the control charts to make the distinction, if any, between an undamaged and an unknown state of the structure.

This paper is organised as follows: Section 2 provides an introduction to change point analysis techniques and the relevant literature is reviewed. This section is followed by a description of the mathematical models and the damage features used in this study, i.e. in Sections 3 and 4, respectively. Section 5 presents the test specimen and the experiment conducted to verify the proposed damage identification and localisation techniques whose results are shown in Section 6. Finally, the paper is concluded in Section 7 with a comparison of the performance of all the models, damage features and statistical tests implemented in this study.

2. Change point analysis

Choosing an effective damage feature is crucial for damage detection analysis. These features can be used in control statistics for damage detection and localisation because such statistics can monitor a change in a process. Once a significant change is encountered in a process, the control statistic can capture this change with the use of a threshold value. It is important in several industrial applications, as well as civil engineering, to know if a change in a process is due to random variations of the measurements over time and the process is still in control, or if the process is out of control due to an assignable cause: in the case of civil engineering systems, a damaging event. Control charts utilise a threshold to distinguish between the two. Once the threshold value is crossed, the process can be deemed out of control. These charts can be used to compare the choice of damage-sensitive features in damage detection schemes because different features will have different sensitivities and produce different damage detection and localisation results. This study presents the effectiveness of several damage features extracted from different mathematical models in data-driven structural damage detection using two-sample control statistics as a means for comparison.

There are several types of control statistics that can be used for change point detection in different processes (Amiri & Allahyari, 2011). They can be used to detect a single change or multiple changes in the mean or variance of the data. One of the first charts generated, the standard univariate Shewhart $\bar{X}$ control chart, was introduced in 1924 by Walter Shewhart to detect a change in the mean of a population (Wilcox, 2003). Since then, control schemes have found widespread application in different disciplines and become more effective. Fugate, Sohn, and Farrar (2001) show an example of application of Shewhart control chart in damage detection of a concrete bridge column. One major flaw in using univariate control statistics is that they can only monitor one variable at a time. If one were to observe a set of quality characteristics that have components with the potential to be interrelated, the univariate control schemes become obsolete. Although it could be argued that univariate control charts could be applied independently to each component of the multivariate data, misleading results may be obtained in some cases due to failure to allow for the inherent relationship among the components of the multivariate data (Zamba & Hawkins, 2006). Therefore, in this paper, multi-dimensional damage features are condensed into a single feature to develop univariate control statistics.

One control chart used in this study is a likelihood ratio test (LRT) of which there are many types. Srivastava and Worsley (1986) propose a form of the LRT that is more effective in detecting a shift involving only the mean vector, while other researchers present improved LRT-based statistical methods capable of detecting shifts in the mean and variance of a vector of observations (Hawkins & Zamba, 2005; Sullivan & Woodall, 1996; Zhang, Zou, & Wang, 2010; Zhou, Luo, & Wang, 2010). Zou, Zhang, and Wang (2006) present a control chart based on change point models for monitoring the intercept, slope or standard deviation of the linear profiles, and name the proposed

method the standardised LRT. The literature related to application of such change point techniques for structural damage detection is scarce (El-Ouafi Bahlous, Abdelghani, Smaoui, & El-Borgi, 2007). This paper uses the normalised likelihood ratio test (NLRT) from Sullivan and Woodall (1996), which has not been used in SHM schemes. The details of this method are presented in Section 2.1.

Another change point analysis used in this paper is based on a two-sample *t*-test; a form of statistical hypothesis testing to distinguish significant differences in the means of two sets of data. Montgomery and Loftis (1987) show the applicability of this *t*-test for detecting trends in water quality variables. In addition, Hawkins and Zamba (2005) use the *t*-test in conjunction with the generalised LRT in order to distinguish between a shift in the mean and the variance in a gold mining quality control example. In effect, there are many different variations of such statistical tests that can be used based on different initial assumptions about the mean and variance of the data. For example, the Satterthwaite–Welch method (Welch, 1947) is used with the assumption that the variance of the two populations is unknown and unequal. However, in this paper, the Student's *t*-test is used in which it is assumed that the variance of the two populations is unknown but equal.

2.1. *Change point analysis using NLRT*

The NLRT can detect a shift in the mean and/or variance of a data-set. It assumes that there are m independent observations that are normally distributed with mean μ and standard deviation σ. If a process is in control, at any partition of the data, the two sets would have similar means and variances. However, if there was a change in the process, the means and variances of the two subgroups would vary substantially from one another.

As explained in Sullivan and Woodall (1996), the log of the likelihood function for the first m_1 observations can be written as

$$l = -\frac{m_1}{2}\log[2\pi\sigma^2] - \frac{m_1\widehat{\sigma_1}^2}{2\sigma^2} - \frac{m_1(\bar{x}_1-\mu)^2}{2\sigma^2}, \qquad (1)$$

in which $\bar{x}_1$ and $\widehat{\sigma_1}^2$ represent the mean and variance of the first m_1 observations, while μ and σ represent the population mean and variance. This function can be maximised to generate l_1 presented as follows:

$$l_1 = -\frac{m_1}{2}\log[2\pi] - \frac{m_1}{2}\log\left[\widehat{\sigma_1}^2\right] - \frac{m_1}{2}. \qquad (2)$$

This procedure can be repeated for the remaining $m_2\,(= m - m_1)$ observations to find the maximum value of the likelihood function, l_2. In this way of partitioning the process into m_1 and m_2, there is an assumption that there is a change in the data at point $m_1 + 1$. However, if this were not the case and the process was in control for all m observations, the likelihood function would be maximised using $\bar{x}$ and $\widehat{\sigma}^2$, the mean and variance of all m observations. This would generate l_o, the maximum of the likelihood function for an assumed in-control process. If l_a, the sum of l_1 and l_2, is much larger than l_o, the process is deemed to be out of control. For this reason, the LRT detects the significance of the difference between the two. It is defined as $\mathrm{LRT}[m_1, m_2] = -2(l_o - l_a)$ and has an asymptotic chi-squared distribution (χ^2) with two degrees of freedom (Sullivan & Woodall, 1996).

This statistics is normalised to create the NLRT with a threshold value of unity. In normalising the statistic in this damage detection scheme, any value of the likelihood ratio (LR) for a damage feature that is above one represents an out of control feature. This can then be correlated to a location on a structure if the damage feature originated from data taken from a localised sensor network. In order to normalise the statistics, it is divided by its expected value (E), based on the dimensionality of the observations, p, and an upper control limit (UCL) based on a desired overall in-control false alarm probability, ω. As explained in Sullivan and Woodall (1996), the in-control expected value is not the same for all values of m_1. If m_1 or m_2 is small, the expected value is larger than when both are the same. When the model order is 1, the expected value can be approximated by simulation or as follows:

$$E = 2\left[\frac{m_1 + m_2 - 2}{(m_1 - 1)(m_2 - 1)} + 1\right]. \qquad (3)$$

The test statistics is also normalised using an UCL which is usually set to give a specified in-control average run length. Based on number of observations and selected confidence level, the UCL can be approximated. Its value has been tabulated in Sullivan and Woodall (1996) using

$$\mathrm{UCL} = \frac{1}{1.7}F^{-1}[(1-\omega)^{1/k^*}], \qquad (4)$$

where $k^* = -4.76 + 3.18\mathrm{Ln}(m)$, while F denotes the cumulative distribution function of a χ^2 distribution with two degrees of freedom. In this implementation, the vector of damage features is successively tested using NLRT (starting from $m_1 = 2$, to avoid numerical instability, through $m_1 = m - 2$) to detect the timing and location of the potential structural damage.

2.2. *Change point analysis using Student's* t*-test*

The other change control threshold that is utilised in this paper is based on the Student's *t*-test. The two-sample *t*-test is a common procedure for testing the differences

between the means of two samples (Montgomery & Loftis, 1987). There are three assumptions that this Student's t-test follows: (1) samples come from a parent population that is normally distributed, (2) the two sample groups are from populations with equal variances and (3) sample observations are independent. The statistics of this test has $N-2$ degrees of freedom (N being the combined length of the two sample vectors) and is given by

$$t = \frac{\bar{X}_1 - \bar{X}_2}{S_p\sqrt{(1/n_1)+(1/n_2)}}, \tag{5}$$

where the variables $\bar{X}_1$ and $\bar{X}_2$ are the means, n_1 and n_2 are the size of the two samples and S_p represents their pooled standard deviation equal to

$$S_p^2 = \frac{(n_1-1)S_1^2+(n_2-1)S_2^2}{(n_1+n_2-2)}, \tag{6}$$

and S_1 and S_2 are the sample standard deviations.

This method, used for cases in which the variance is assumed to be unchanged, can be used with linear regression parameters. This is because it represents the realistic condition when a property of the structure is changed due to damage if the change does not affect the estimation uncertainty of the damage feature. In this paper, this two-sample t-test is applied sequentially through the vector of damage features to identify and localise the structural damage.

UCL and lower control limit (LCL) for this test are then calculated using the Student's t inverse cumulative distribution function at a certain confidence level $(1-\omega)\%$ and $N-2$ degrees of freedom ($N = n_1 + n_2$) based on

$$\mathrm{UCL} = t_{(1-(\omega/2)),N-2}, \quad \mathrm{LCL} = t_{\omega/2,N-2}. \tag{7}$$

3. Localised damage detection method: mathematical models

There are many different parameters that can be used as damage-sensitive features in control charts. Ghosh, Datta, Kim, and Sweeting (2006) use the ratio between two different univariate linear regression coefficients on a parallel-line assay. In order to find and use dynamic characteristics of a structure as damage features, Huang (2001) proposes a procedure that uses the multivariate autoregressive (M-AR) vector model for numerical simulations of a six-storey shear building subjected to white noise and low-pass filtered white-noise input, while simulated acceleration and velocity responses were used in separate scenarios to study the effect of signal type.

Similarly, He and De Roeck (1997) use M-AR to find the modal parameters of a water transmission tower from measured acceleration responses during ambient vibration. Furthermore, Hung, Ko, and Peng (2004) identify modal parameters from measured input and output data using a vector backward autoregressive with exogenous (ARX) model. This method was experimentally validated using measured acceleration responses of a five-storey scaled steel frame under a shake table test. Zheng and Mita (2007) fit autoregressive moving average (ARMA) models to the time series of acceleration responses of the structure and use the distance between the ARMA models to detect the existence of the damage, which is consequently localised by minimising the cross-correlation of multiple excitations through pre-whitening filtering.

Gul and Catbas (2011) create ARX models based on acceleration responses of different sensor clusters of the healthy structure, and these models are used for predicting the data from the damaged structure, while the difference between the fit ratios are used as damage-sensitive features. Effectiveness of AR models are investigated in several other studies by using the time history of acceleration responses of the system to generate damage indicators (e.g. De Lautour & Omenzetter, 2010; Dorvash, Pakzad, & Labuz, 2014; Fugate et al., 2001; Nair et al., 2006; Zheng & Mita, 2009); however, there are also successful applications of these models for damage localisation in the literature which use time histories of measured strain signals (Dorvash, Pakzad, Labuz, Ricles, & Hodgson, in press; Noh, Nair, Kiremidjian, & Loh, 2009; Sohn, Farrar, Hunter, & Worden, 2001). While some of these studies use data from real-world systems for validation (Gul & Catbas, 2011; Sohn et al., 2001), most of the proposed damage detection techniques are verified through laboratory testing of specimens with different levels of complexity from retrofitted reinforced concrete column (Fugate et al., 2001) to four-storey two-bay by two-bay steel braced frame (Nair et al., 2006).

The damage features studied in this paper come from the linear regression coefficients produced by an algorithm called influenced-based damage detection algorithm (IDDA) developed by Dorvash et al. (2014, in press). These damage features are shown to be viable ways of detecting damage in a structure because they are sensitive to the changing properties of a structure. The IDDA correlates the response [measured acceleration signals in Dorvash et al. (2014) and measured strain signals in Dorvash et al. (in press)] of a structure at various locations by creating influence coefficients from a linear regression model based on output of a dense sensor network. When damage occurs, the relationship between responses changes, which will be reflected in the influence coefficients and indicate the existence of damage. The location can then be pinpointed by correlating such data-driven damage features to the location of the sensors.

3.1. SVR model

The simplest linear mapping model is the SVR model. It relates the acceleration response of one location to another location at the current time step. This version of the model can be represented using

$$y_j = \alpha y_i + \beta + \epsilon, \tag{8}$$

which correlates the response at node j to current response at node i through α with intercept β and error ϵ. Since the effects of previous time steps are removed from this equation, the intercept (β) is added into Equation (8) to account for the initial conditions. The influence coefficient α is then used to extract damage feature from the linear regression model in this study.

The derivation and validation of this simplified mathematical model can be found in Dorvash et al. (2014) on a scaled beam–column connection. Since this damage feature has already been proven to detect and localise damage in small- and large-scale structural models (Dorvash et al., 2014, in press), it is used as a basis for comparison and derivation of the proceeding damage features discussed in the following sections.

3.2. AR and ARX models

The SVR model can be expanded to include more information about the system from past and present time steps of the structural response. In effect, this ARX model can be written as follows:

$$y_j(n) + \sum_{p=1}^{P} \alpha_{jp} y_j(n-p) = \sum_{q=0}^{Q} \alpha_{iq} y_i(n-q) + \varepsilon(n), \tag{9}$$

where y_j and y_i are outputs at locations j and i, respectively; α_{jp}'s and α_{iq}'s are the ARX coefficients; $\varepsilon(n)$ represents the residuals; n is the time index and P and Q are orders of the AR and exogenous parts of the ARX model, respectively. Derivation and validation of this formulation can be found in Yao and Pakzad (2012).

This ARX model can be simplified to just include one location on a structure. This regression may produce more localised results if only one location is involved in the model. Acceleration response at the same location in time can be established using an AR model as follows:

$$y_j(n) = \sum_{p=1}^{P} \alpha_p y_j(n-p) + \varepsilon(n). \tag{10}$$

In this formulation, y_j is the output at location j, α_p's are AR coefficients, $\varepsilon(n)$ represents the residuals, n is the time index and P is the order of the AR model. In this study, the regression coefficients (α_p's, α_{jp}'s and α_{iq}'s) are used to generate damage-sensitive features from the AR and ARX linear regression models to be tested in the change point analyses.

The order of the AR and ARX models must be determined before the influence coefficients can effectively be used in damage control charts. The accuracy of the two regression models depends on the selected model orders based on the data from the localised sensor networks. While higher model orders, in general, deliver more details of the system and reduce the estimation bias, it is always desired to keep the order at the minimum level to avoid over-parameterisation. One way to establish the model order is to minimise the Akaike's information criterion (AIC) which is used in Friedlander and Porat (1984) and Figueiredo et al. (2011) as follows:

$$\mathrm{AIC}(p) = (L-p) \times \mathrm{Ln}(\mathrm{SE}) + 2p, \tag{11}$$

where p is the number of parameters in the AR model and SE is the sum of the regression residuals divided by $L - p$ (L being the total number of data samples). Once the model order number is found and the AR and ARX coefficients are regressed, their coefficients are condensed to generate a univariate control statistics. Section 4 explains the condensation methods adopted in this paper.

3.3. CR model

The SVR model can also be modified to correlate three locations on a structure without over parameterising the system. This model is called the CR model. There are many different types of regressors that can be used in CR models. For this implementation, y_i in Equation (8) is changed to the average of two outputs. In effect, the mathematical model would be calculated as

$$y_k = \alpha_{ijk} \frac{(y_i + y_j)}{2} + \beta + \epsilon, \tag{12}$$

in which an additional location's acceleration output, y_k, can be included to create the new coefficient α_{ijk}. The effectiveness of CR influence coefficient is analysed and compared to the AR, ARX and SVR model parameters presented above in the structural damage detection based on change point analysis.

4. Localised damage detection method: damage features

There are two types of features that are used to test the null hypothesis that the mean of the two observation samples from different states of the system is equal. The first of these is a scalar function of the regression coefficients – referred to as *Alpha-based Coefficients* in this paper – obtained from the regression models discussed earlier. In cases of the SVR and CR models, the output of this

function is the influence coefficients themselves, whereas for the AR and ARX models, the Mahalanobis distance is utilised to find a scalar representation of the multivariate regression coefficients corresponding to a condition of interest and those corresponding to a reference condition (Mosavi, Dickey, Seracino, & Rizkalla, 2012). The Mahalanobis distance of vector x can be computed by using

$$D_{\mathrm{m}}(x) = \sqrt{(x-\mu)^{\mathrm{T}} S^{-1} (x-\mu)}, \tag{13}$$

with reference to the matrix of the baseline regression coefficients with mean μ, and S is its covariance matrix. Once the distances are calculated, these scalar representations of the influence coefficients are used in the change point analysis.

The second damage feature used in this study is called the *Angle Coefficient*. This coefficient measures the angle between regressed lines from two different states of the system. In other words, for damage detection methods, instead of measuring the difference in slope between a healthy state line and an unknown state line of a structure, the angle between the two lines can be compared to detect change as well. In effect, the *Angle Coefficient* can be written as follows:

$$\Gamma = \cos^{-1}\left|\frac{v \times v'}{\|v\|\|v'\|}\right| = \cos^{-1}\left|\frac{\alpha\alpha' + 1}{\sqrt{\alpha^2+1}\sqrt{\alpha'^2+1}}\right|, \tag{14}$$

where v and v' correspond to a vector $[-1, \alpha]^{\mathrm{T}}$ for an undamaged state and a vector $[-1, \alpha']^{\mathrm{T}}$ for an unknown state, respectively. In this formulation, α and α' are the respective influence coefficients from SVR or CR models. For ARX and AR models (with model order p), $v = [-1, \alpha_1, \alpha_2, \ldots, \alpha_{2p+1}]^{\mathrm{T}}$ and $v = [-1, \alpha_1, \alpha_2, \ldots, \alpha_p]^{\mathrm{T}}$, respectively.

These two sets of coefficients, *Alpha-based Coefficients* and *Angle Coefficients*, are extracted from the acceleration signals measured from a baseline and an unknown state. They are then tested for a change in their mean using the NLRT or t-test method discussed in Section 2.

5. Test set-up

A two-bay steel tube frame test bed was constructed at the laboratory of Advanced Technology for Large Structural Systems at Lehigh University. In this paper, the specimen is used to analyse the effectiveness of the damage features discussed above. This frame was built as a test bed for damage detection, mainly to represent typical building frames or bridge girders. It has nine interchangeable sections, 0.2 m in length, that can be changed throughout the frame in order to simulate damage. These interchangeable sections have different cross-sectional properties than the healthy state (shown in Table 1) which correspond to 20% reduction in member stiffness. In order to simulate a realistic damage scenario, the length of these switchable members was designed so that a negligible change would occur in the global behaviour of the frame pre- and post-damage. Figure 1 shows the experimental set-up used in this study.

Table 1. Geometry of baseline and interchangeable sections.

Feature	Baseline sections	Interchangeable 'Damage' sections
Outer dimension of hollow cross section	0.05 m	0.05 m
Tube thickness	2.16 mm	1.65 mm
Cross-sectional area	410.57 mm^2	324.57 mm^2
Moment of inertia	162,526 mm^4	130,811 mm^4

In order to collect data, the specimen was instrumented with 21 wired accelerometers, labelled in Figure 2 with L, C or R on left, centre and right portions of the frame. During testing, there were a total of 40 runs of data collected. For each run, the sampling rate was 500 Hz and 1000 samples were recorded so that each test lasted a total of 2 s. The first 20 runs were taken when the frame was in an undamaged state, where the first 10 tests of this group serve as a known healthy baseline for comparison throughout this paper. The Mahalanobis distance between these first 10 healthy runs and the next 10 healthy runs creates a baseline distance for comparison. It was at this point (run 21) that damage was simulated for the second half of the experiment.

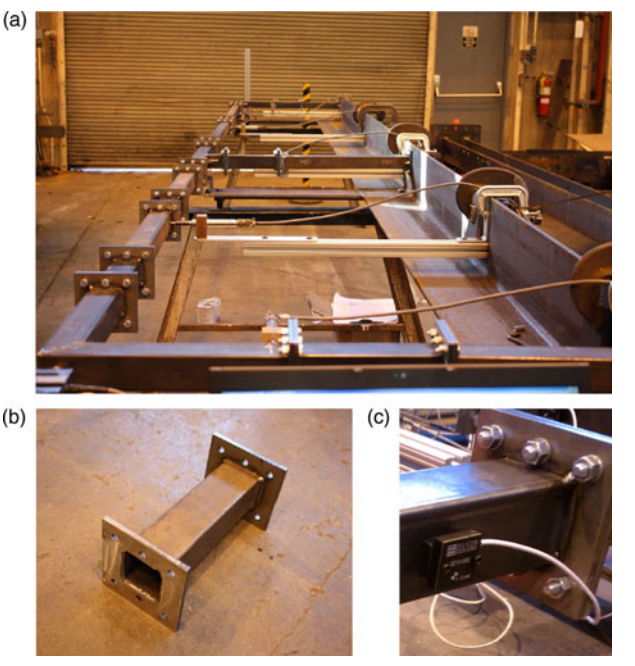

Figure 1. Experimental set-up: (a) scaled frame, (b) switch-out member and (c) wired accelerometer.

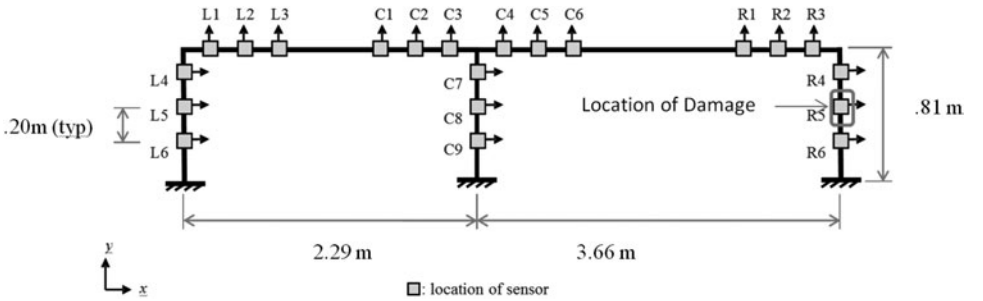

Figure 2. Sketch of the specimen and the location of the introduced damage.

For this study, the damage case consists of replacing a healthy section with one of less stiffness at the location of sensor R5, which corresponds to less than a 1% change in the lateral stiffness as well as the first three natural frequencies of the frame. After this section is exchanged, an additional 20 tests were taken. These tests will serve as the unknown state of the structure after a damaging event by comparing the Mahalanobis distance between these 20 'damaged' runs and the baseline distance from the healthy start runs. The results, shown in Section 6, should detect the timing of the damage after the 20th test and localise it to the right column of the frame.

There are two sets of data collected, which represent measurements that would be taken pre- and post-damaging event or regular maintenance of a structure. Therefore, it is possible to assume that the structure behaves linearly during data collections. In addition, Dorvash et al. (2010) show that the type of excitation used with IDDA does not affect the detection of damage. In order to dynamically excite the frame, impact loading is chosen as the excitation method for this implementation. This excitation is similar to ambient vibration in not imposing any specified excitation frequency to the frame. The impact amplitude was limited to ensure that the linear behaviour assumption for the experimental frame holds. Therefore, the acceleration response of frame is recorded while the frame is struck with a hammer on the right column and the frame freely vibrates on its own.

The data from this experiment were previously used in Nigro, Pakzad, and Dorvash (2014) to investigate the performance of IDDA damage features using a change point framework, where statistics such as univariate cumulative sum (CUSUM), exponentially weighted moving average (EWMA), mean square error (MSE), modified MSE, Mahalanobis distances and Fisher criterion are used. As stated, in this paper two-sample change point statistics are implemented for different combinations of damage features and regression models.

6. Results

As shown in Figure 2, the damage case in question for this study includes damage at a section on the right side column; therefore, the results should detect damage at or near this location. Three sensor clusters on the left, centre and right portions of the frame are used for damage detection. It should be noted that the data measured with sensors L1, C3, C5 and C9 were excluded from the damage detection process, as the preliminary inspection of the measured signals revealed faulty behaviour of these sensors.

Considering there are five or six sensors in each sensor group, there are many different combinations of sensors that can be paired in the different linear regression models. Therefore, only sensors within the same cluster will be paired with one another. In effect, for a sensor cluster consisting of six sensors, in cases where two sensor nodes are paired with one another, 30 pairs can be made without pairing a sensor with itself. This occurs in SVR and ARX linear models. However, based on the CR model, 120 different combinations can be made. This section presents the results of the damage detection techniques of Section 2 using the regression models and damage features introduced in Sections 3 and 4.

6.1. *SVR results*

The coefficients made using SVR model are readily used in the NLRT and *t*-test. Since the *Angle Coefficients* are found in reference to the first baseline run of the experiment, a possible damage point should be detected when both damage features are split into two groups of 20 tests. Figure 3 presents the LR and absolute *t*-statistics of the *Alpha-based* and *Angle Coefficients* in this case. All these plots show peaks on the split at run number 20 which implies the possible timing of the damage. These peaks correspond to the maximum test statistics; since the *t*-test or LRT statistics are sequentially created for every two partitions of the observations as a means to signify the difference between two partitions, these statistics are maximised when all the observations in each partition belong to one state (healthy or damaged) of the system. For *Alpha-based* and *Angle Coefficients* extracted from SVR models, this corresponds to splitting observations at run number 20.

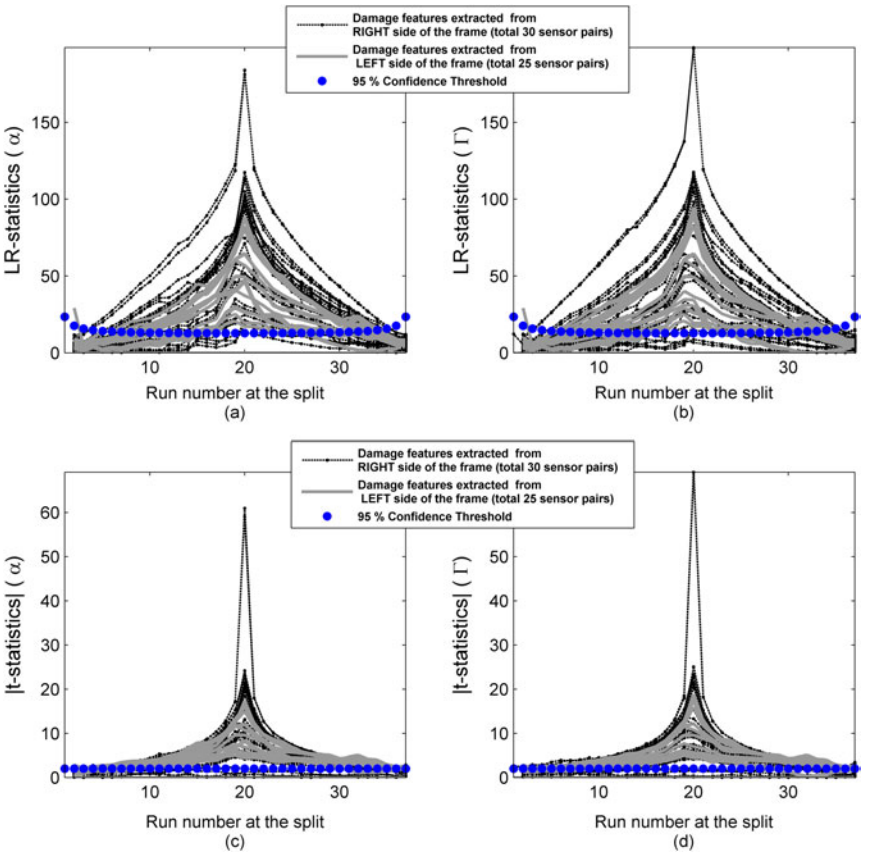

Figure 3. Test statistics of the damage features extracted from the SVR models: (a) LRT statistics, Alpha-based Coefficients; (b) LRT statistics, Angle Coefficients; (c) absolute *t*-statistics, Alpha-based Coefficients and (d) absolute *t*-statistics, Angle Coefficients.

The change detection threshold is also plotted for both tests in these plots. It is seen that when run number at the split is 20, the extracted damage features from left and right side of the frame cross the change threshold, and this identifies the occurrence of damage at the 21st run of the experiment. The damage features extracted from the left and right sensor clusters at this split are plotted in Figure 4. As the entire frame's response is changing with the switch of the damaged section, it is expected that the damage features on the left side also cross the change threshold. However, the detected change at the right side of the frame is more pronounced than the left side. This implies that with a sensor located at right or left side of the frame, the occurrence of the damage is most likely successfully identified; however, localising the damage to a specific location on the frame requires denser instrumentation.

The average of the test statistics associated with each sensor location that indicates a statistically significant change in the extracted damage features is used in order to localise the identified damage. This quantity correlates the severity of the change in the damage features with the sensor locations on the structure. Figure 5 depicts these localised damage indicators extracted from the SVR models. This figure shows that based on the maximum averaged test statistics, damage is localised to R6. With this measure, the actual location of the damage R5 has the second largest damage indicator. Therefore, it can be concluded that this change detection method successfully localises the damage to its true locale.

6.2. *ARX model results*

The regression coefficients of ARX models, with model order 4, are first condensed into a scalar damage feature using Mahalanobis distance which is then used in the developed damage detection methods. The model order selection in this implementation is based on the AIC described in Section 3.2 along with the fact that the first 10 test runs are assumed to be conducted on a known healthy structural configuration, and thus are used as reference to calculate the Mahalanobis distances.

Therefore, Mahalanobis distances are calculated between coefficients from the first 10 healthy state runs and the last 10 healthy state runs. This step creates a baseline distance. Then, the first 10 healthy runs and the 20 damaged runs are used to create a distance to compare to the reference. The distances calculated in the latter coefficients should be bigger than the baseline condition at

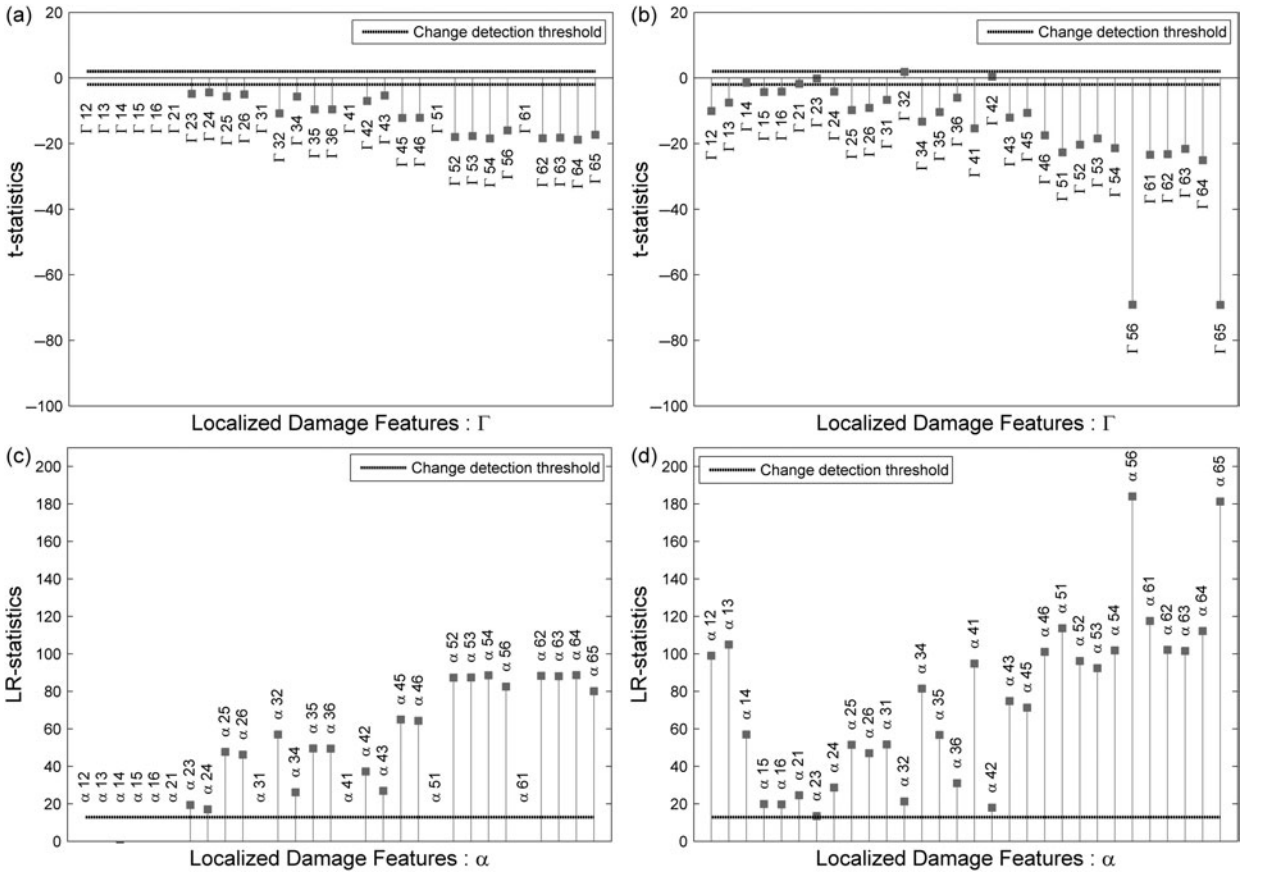

Figure 4. Test statistics of the damage features extracted from the SVR models (split at the 20th run): (a) Angle Coefficients at the left side; (b) Angle Coefficients at the right side; (c) Alpha-based Coefficients at the left side and (d) Alpha-based Coefficients at the right side.

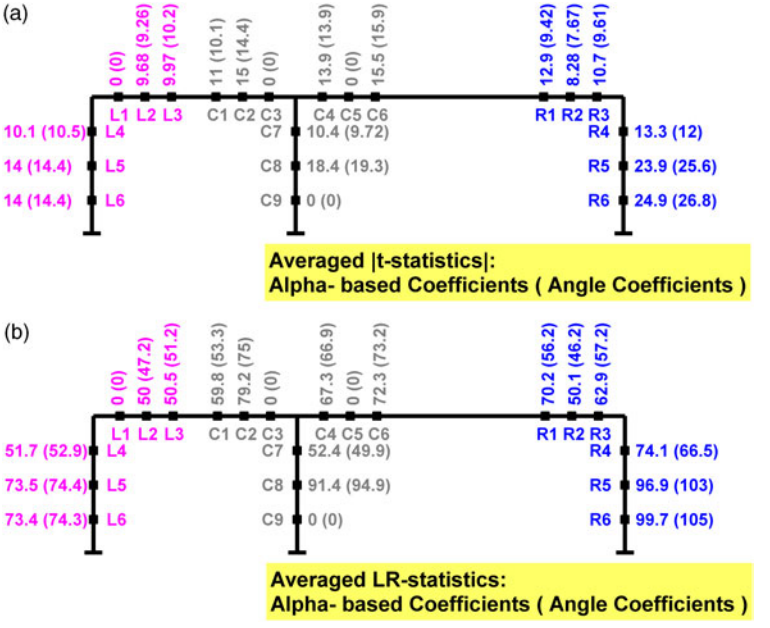

Figure 5. Localised damage indicators using SVR models: (a) averaged absolute *t*-statistics and (b) averaged LRT statistics.

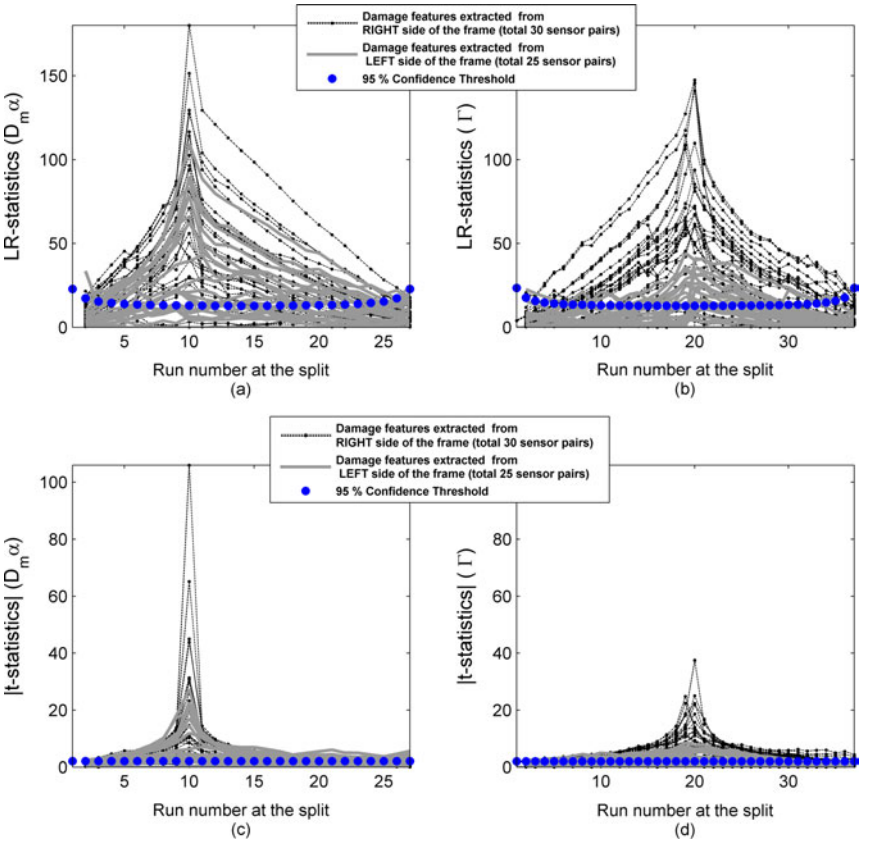

Figure 6. Test statistics of the damage features extracted from the ARX models: (a) LRT statistics, Alpha-based Coefficients; (b) LRT statistics, Angle Coefficients; (c) absolute *t*-statistics, Alpha-based Coefficients and (d) absolute *t*-statistics, Angle Coefficients.

areas of damage. In effect, a possible significant change is expected to happen when the run number at the split is 10. As the proposed *Angle Coefficients* are scalar quantities, no preprocessing is required prior to the change point analysis, and therefore the timing of possible damage is expected to be detected at the split with run number 20. Figure 6 shows the test statistics of the features extracted from ARX models. This figure shows that the damage features from the ARX model do identify the correct timing of damage.

The damage features at the identified change time are plotted in Figures 7 and 8. These figures show that, similar

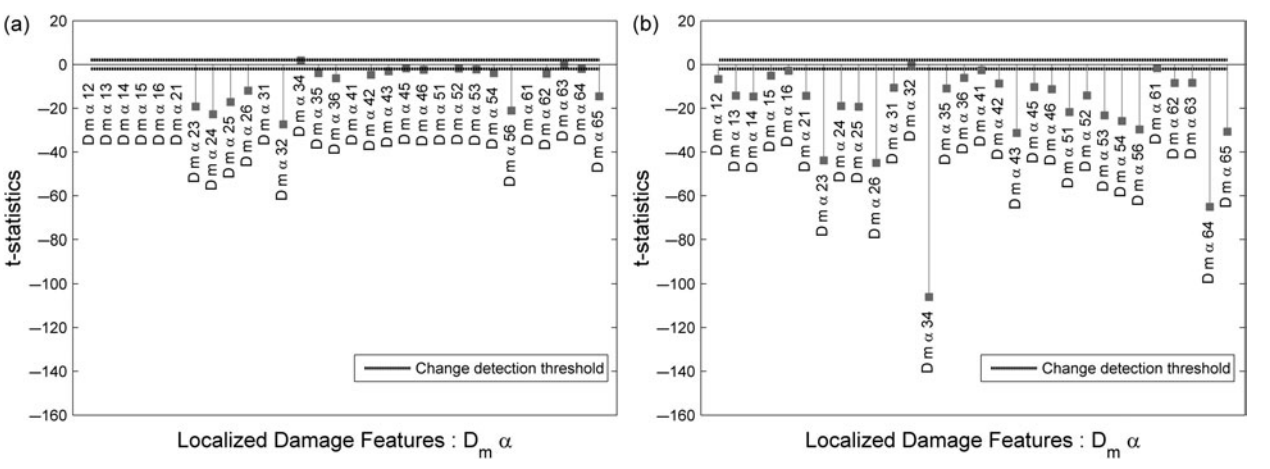

Figure 7. The *t*-statistics of the Alpha-based Coefficients extracted from the ARX models (split at 10th run): (a) at the left side and (b) at the right side.

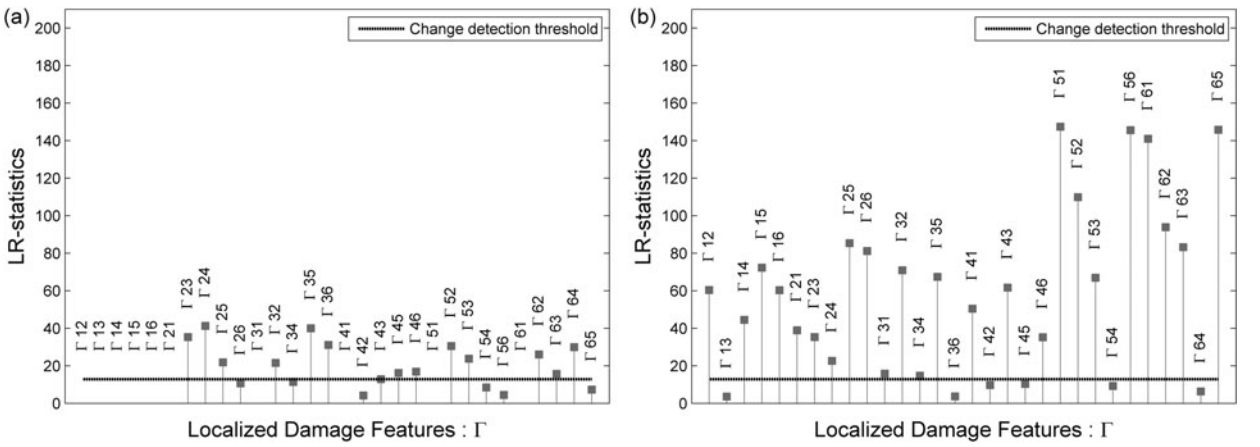

Figure 8. The LRT statistics of the Angle Coefficients extracted from the ARX models (split at 20th run): (a) at the left side and (b) at the right side.

to the SVR results, at time of the damage (11th run in case of *Alpha-based coefficients* and 21st run based on *Angle Coefficients*), several coefficients on the left and right side of the girder cross the change threshold. The test statistics are then analysed for their effectiveness in localising the damage. The results are displayed in Figure 9. This figure shows that the averaged test statistics of the Mahalanobis distance locate the damage at R4, while such damage indicators based on *Angle Coefficients* localise the damage to its true location at R5.

6.3. *CR results*

CR in this implementation involves three different locations. In effect, the results may show a more localised detection of damage because the coefficients themselves include a higher spatial distribution. It is still expected that the coefficients with combinations of the locations on the right-side column will show more significant change than those extracted from the left side of the frame. The results for the *Alpha-based* and *Angle Coefficients* are shown in Figure 10. These plots are initially analysed for the timing of damage.

All plots present a peak when the vector of the coefficients is split at the 20th run of testing. As these peaks occur above the change threshold with 95% confidence level, it can be concluded that this is the correct time of the damaging event. The results can then be analysed for their effectiveness in localising the damage to the right-side column of the frame. Figure 11 shows the

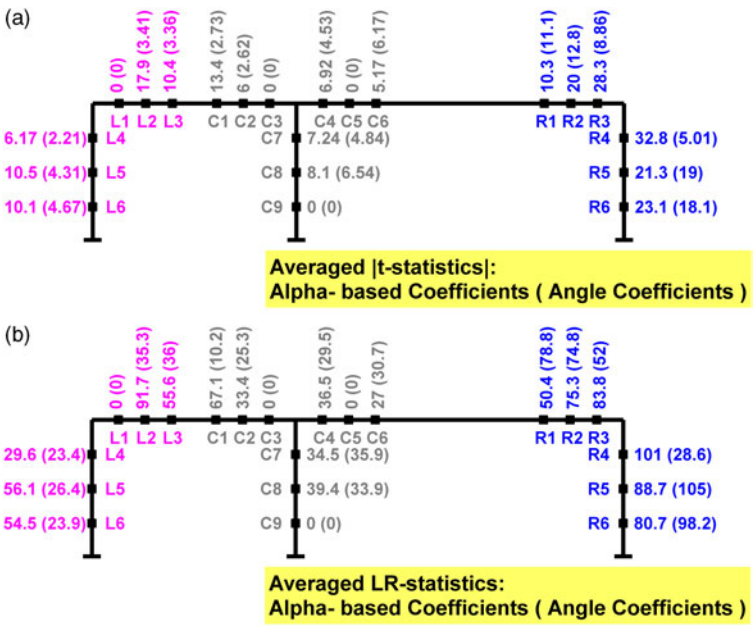

Figure 9. Localised damage indicators using ARX models: (a) averaged absolute *t*-statistics and (b) averaged LRT statistics.

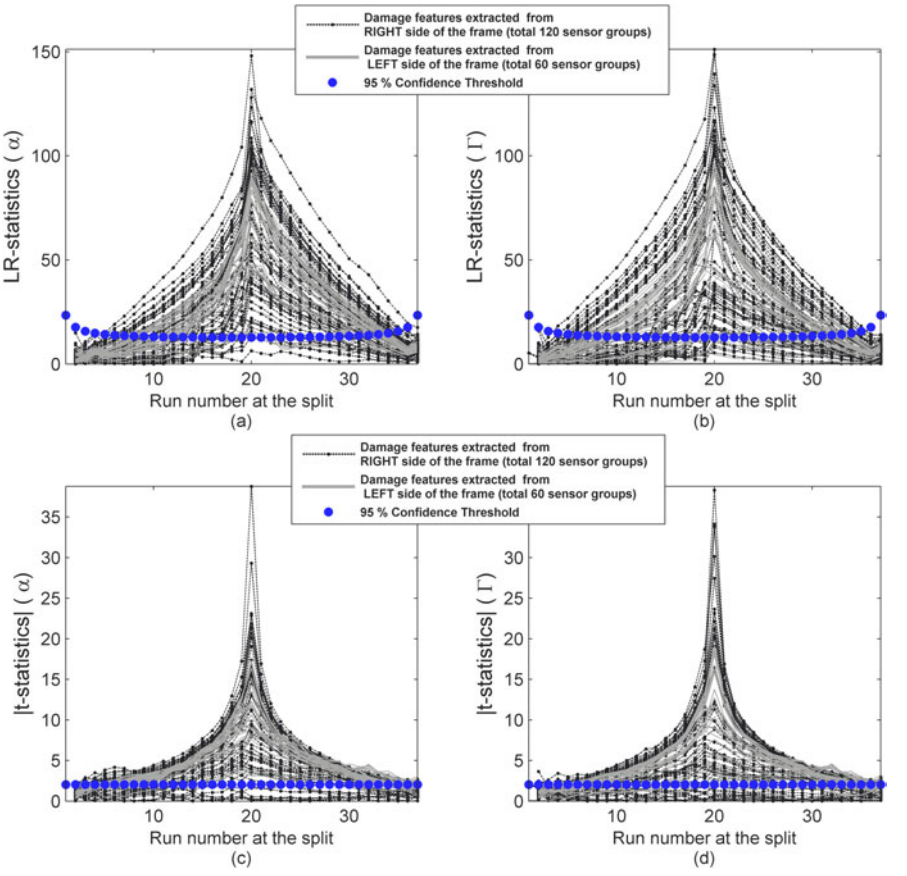

Figure 10. Test statistics of the damage features extracted from the CR models: (a) LRT statistics, Alpha-based Coefficients; (b) LRT statistics, Angle Coefficients; (c) absolute *t*-statistics, Alpha-based Coefficients and (d) absolute *t*-statistics, Angle Coefficients.

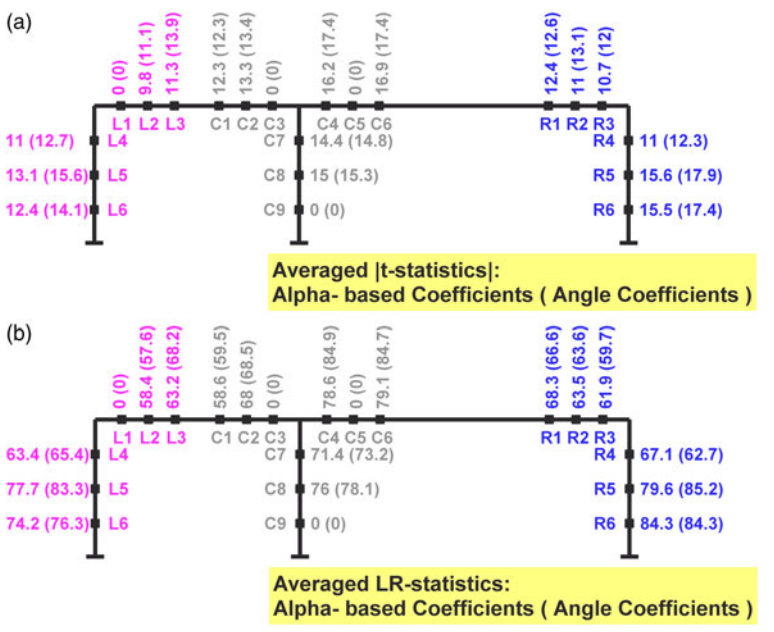

Figure 11. Localised damage indicators using CR models: (a) averaged absolute *t*-statistics and (b) averaged LRT statistics.

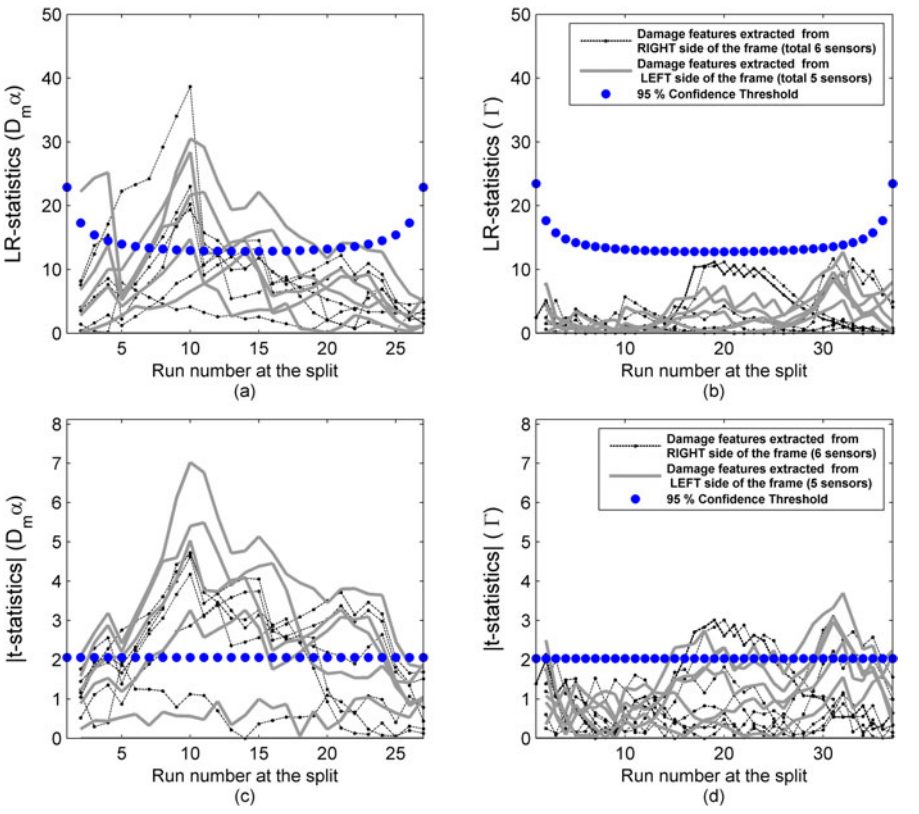

Figure 12. Test statistics of the damage features extracted from the AR models: (a) LRT statistics, Alpha-based Coefficients; (b) LRT statistics, Angle Coefficients; (c) absolute *t*-statistics, Alpha-based Coefficients and (d) absolute *t*-statistics, Angle Coefficients.

localised damage indicators. This figure shows that the *Angle Coefficients* generated from CR models find the true location of the damage (R5) using LRT or Student's *t*-test, while the performance of the *Alpha-based Coefficients* depends on the test statistics; location of the damage is pinpointed to the location of sensor C6 when using *t*-test, and R6 when using LRT.

6.4. AR model results

AR models are also tested in the developed damage detection strategies. The *Alpha-based* and *Angle Coefficients* in this case are generated as for the ARX models. These coefficients are different from those generated based on the ARX models, in that the damage features extracted from the AR models represent one sensor node on the

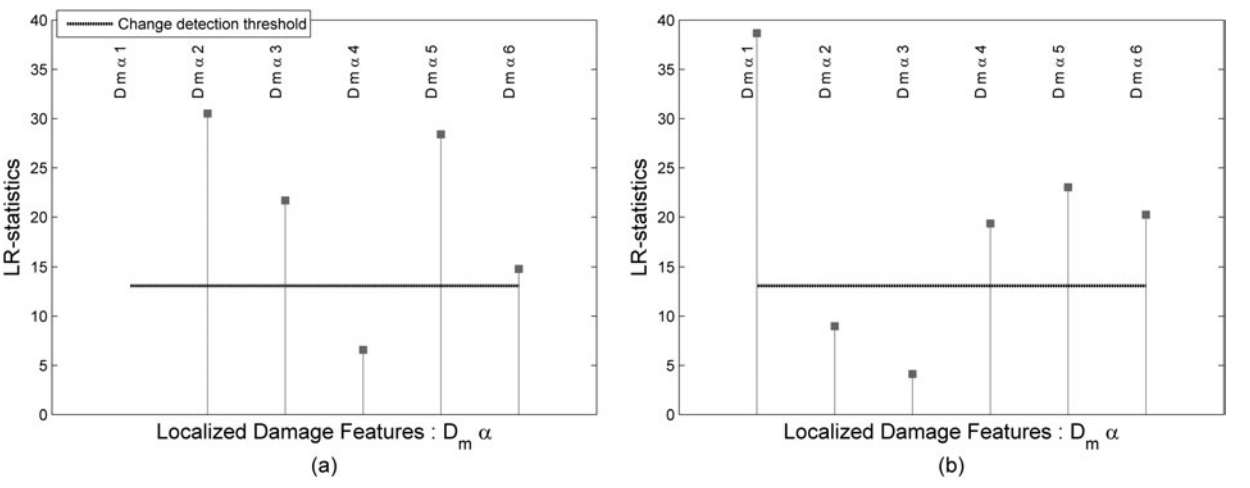

Figure 13. The LRT statistics of the Alpha-based Coefficients extracted from the AR models (split at the 10th run): (a) at the left side and (b) at the right side.

frame. Figure 12 summarises the results of the two-sample change detection on the extracted damage features from AR models. This figure shows that for the AR models, the peaks of the change point test statistics are not as distinct as in the previous cases. While using the Mahalanobis distance, the timing of the damage is detected correctly, and the *Angle Coefficients* are not successful in detecting the time or location of the damage with this model.

The LRT statistics are shown in Figure 13 for *Alpha-based Coefficients* when data is split at 10th run. This figure shows that the extracted damage features are not successful in pinpointing the damage to its true location. This is most likely due to the fact that the simulated damage in this experiment (20% stiffness reduction in a 0.2-m long segment of one of the columns) does not significantly change the natural vibration frequency of the frame as well as the characteristic roots of the AR models extracted from the acceleration response of the frame at different locations. In addition, Yao and Pakzad (2012) showed that estimates of such AR coefficients have low robustness to environmental factors and measurement noise, and therefore to use the AR model for structural damage detection purposes, other damage features such as autocorrelation function of the AR residuals and AR model spectrum are more promising.

6.5. *False detection check*

Prior to concluding that the proposed damage detection methods are viable ways of identifying the structural damage, their false detection quality should also be tested. For this purpose, these methods are applied on a group of 40 runs consists of the first 20 tests on the healthy configuration of the frame combined with a random permutation of these 20 runs. As all the tests are from the same structural condition, it is expected that no damage is detected using the damage-sensitive features in this case.

Figure 14 illustrates the LRT and *t*-statistics extracted from the coefficients of the SVR, ARX, CR and AR models for these 40 sets of data from the undamaged state, along with the change detection threshold corresponding to 95% confidence level. This figure shows that when all the observations belong to one state of system, no large and distinct peaks are evident above the change threshold as in the previous cases. However, it is also seen that some

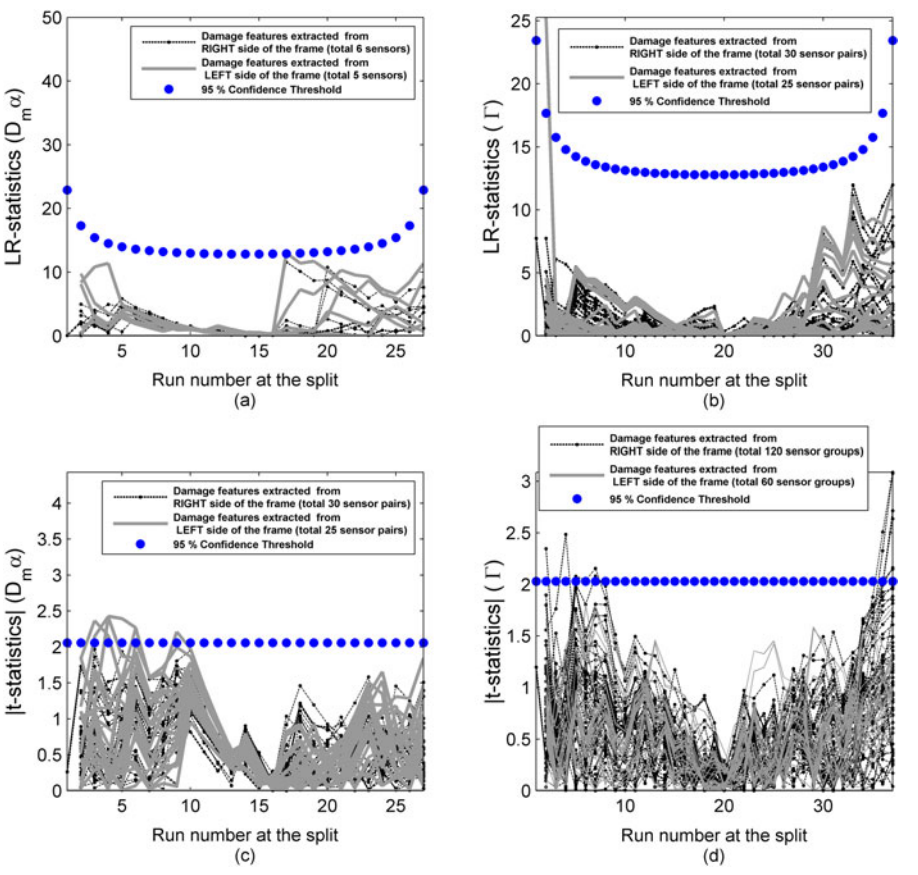

Figure 14. Test statistics of the damage features extracted from different regression models: (a) AR model, LRT statistics, Alpha-based Coefficients; (b) SVR model, LRT statistics, Angle Coefficients; (c) ARX model, absolute *t*-statistics, Alpha-based Coefficients and (d) CR model, absolute *t*-statistics, Angle Coefficients.

Table 2. Summary of the damage identification of the steel girder.

Change point method	Identified damage location[a]			
	t-test		LRT	
Damage features	Alpha-based Coefficients	Angle Coefficients	Alpha-based Coefficients	Angle Coefficients
SVR model	R6	R6	R6	R6
ARX model	R4	R5	R4	R5
CR model	C6	R5	R6	R5

[a] True damage location is R5.

of the statistics do cross the change threshold. This does not signify damage as it is consistence with average false detection of the corresponding tests on observations from a normal distribution at 95% confidence level.

7. Summary and conclusions

This study is concerned with the effectiveness of different damage features and multivariate linear regression models used in data-driven structural damage identification. For this purpose, a successive NLRT and a sequential two-sample *t*-test are adopted to test the change in two different damage-sensitive features based on the regression coefficients of four different linear regression models (SVR, CR, ARX and AR models). This methodology is tested on a scaled two-span frame in which damage is simulated by switching a segment of one of the columns with a section with 20% less stiffness. It was observed that all of the mathematical models were successful in identifying the occurrence of the damage, except when the *Angle Coefficients* from AR models were tested. The location of damage was then identified based on the test statistics from SVR, CR and ARX models.

These results are summarised in Table 2. This table shows that the *Angle Coefficients* have a better performance in localising the damage, as in all cases the simulated structural damage is localised to its true or neighbouring sensor node. *Alpha-based Coefficients*, however, perform less accurate and robust in damage localisation; their damage localisation performance depends on the underlying mathematical model and the change point test statistics. It is also observed that the ARX model has the most accurate localisation estimate regardless of the test statistics used, and its performance is improved in combination with the proposed *Angle Coefficients*.

It should be noted that in any damage detection experimental test bed similar to the one used here, assembly procedure for simulation of damage could change the system and generate misleading results in the change point analysis. To address this issue, note the following: (1) through the presented methods, damage is successfully localised to its true neighbourhood, (2) damage detection methods in this paper are all model-free techniques. Model-based damage detection methods with appropriate parameterisation could have benefits of detecting such changes, and (3) the consistency of the assembly of the test bed was examined in preliminary experiments (not included in the paper) by repeating the experiments in healthy/damaged states. A procedure for the sequence of test bed assembly is established to ensure that the results remain consistent.

Since the false detection quality of the proposed methods was also verified using data-sets from the healthy condition of the structure, it can be concluded that these methods are viable techniques to identify and locate damage in structural systems. It was shown that incorporating multiple mathematical models, damage-sensitive features and change detection tests improve the overall performance of these model-free structural damage detection techniques when impact loading is used to dynamically excite the steel frame. This shows potential application of such methodologies in automated damage localisation during events such as earthquake; however, in order to extend the application of these methods, their performance should also be evaluated using ambient vibration as excitation in future research.

In addition, in this single damage scenario, it was observed that when damage features are developed based on relative change in the acceleration response at nodes inside each sensor cluster, occurrence of damage could be statistically identified even using the data from a sensor that is located relatively far from the damaged member. This implies that these methods are most likely capable of detecting the timing of damage in multiple damage scenarios as well. However, damage localisation in such scenarios – which is a well-known problem in the SHM field – is outside the scope of this paper and further research is required to validate the performance of these techniques in more complex damage scenarios.

Acknowledgements

Financial support of National Science Foundation and Commonwealth of Pennsylvania, Department of Community and Economic Development is gratefully acknowledged.

Funding

Research funding is partially provided by the National Science Foundation [grant number CMMI-0926898] through Sensors and Sensing Systems Programme, and by a grant from the Commonwealth of Pennsylvania, Department of Community and Economic Development, through the Pennsylvania Infrastructure Technology Alliance (PITA).

Notes

1. Email: malloryybeth@gmail.com
2. Email: pakzad@lehigh.edu
3. Email: pycpyc1988@hotmail.com

References

Alvandi, A., & Cremona, C. (2006). Assessment of vibration-based damage identification techniques. *Journal of Sound and Vibration*, *292*, 179–202.

Amiri, A., & Allahyari, S. (2011). Change point estimation methods for control chart post signal diagnostics: A literature review. *Quality and Reliability Engineering International*, *28*, 637–685.

Bodeux, J., & Golinval, J. (2003). Modal identification and damage detection using the data-driven stochastic subspace and ARMAV methods. *Mechanical Systems and Signal Processing*, *17*, 83–89.

Cruz, P.J.S., & Salgado, R. (2009). Performance of vibration-based damage detection methods in bridges. *Computer-Aided Civil and Infrastructure Engineering*, *24*, 62–79.

De Lautour, O.R., & Omenzetter, P. (2010). Nearest neighbor and learning vector quantization classification for damage detection using time series analysis. *Structural Control and Health Monitoring*, *17*, 614–631.

Deraemaeker, A., & Preumont, A. (2006). Vibration based damage detection using large array sensors and spatial filters. *Mechanical Systems and Signal Processing*, *20*, 1615–1630.

Doebling, S.W., Farrar, C.R., & Prime, M.B. (1998). A summary review of vibration-based damage identification methods. *Shock and Vibration Digest*, *30*, 91–105.

Dorvash, S., Pakzad, S.N., Labuz, E., Chang, M., Li, X., & Cheng, L. (2010). Validation of a wireless sensor network using local damage detection algorithm for beam–column connections. In *Proceedings of SPIE: Proceedings of the SPIE Sensors and Smart Structures Technologies*, San Diego, CA (Vol. 7647, pp. 764719-1–764719-11). doi: 10.1117/12.847581

Dorvash, S., Pakzad, S.N., & Labuz, E.L. (2014). Statistics based localized damage detection using vibration response. *Smart Structures and Systems*, *14*. doi: 10.12989/sss.2014.14.2.000

Dorvash, S., Pakzad, S.N., Labuz, E.L., Ricles, J.M., & Hodgson, I.C. (in press). Localized damage detection algorithm and implementation on a large-scale steel beam-to-column moment connection. *Earthquake Spectra*. doi: http://dx.doi.org/10.1193/031613EQS069M

El-Ouafi Bahlous, S., Abdelghani, M., Smaoui, H., & El-Borgi, S. (2007). A modal filtering and statistical approach for damage detection and diagnosis in structures using ambient vibrations measurements. *Journal of Vibration and Control*, *13*, 281–308.

Farrar, C.R., Baker, W.E., Bell, T.M., Cone, K.M., Darling, T. W., Duffey, T.A., Eklund, A., & Migliori, A. (1994). *Dynamic characterization and damage detection in the I-40 bridge over the Rio Grande* (Report LA-12767-MS). Los Alamos, NM: Los Alamos National Laboratory.

Figueiredo, E., Figueiras, J., Park, G., Farrar, C.R., & Worden, K. (2011). Influence of the autoregressive model order on damage detection. *Computer-Aided Civil and Infrastructure Engineering*, *26*, 225–238.

Friedlander, B., & Porat, B. (1984). The modified Yule-Walker method of ARMA spectral estimation. *IEEE Transactions on Aerospace and Electronic Systems*, *AES-20*, 158–173.

Fugate, M.L., Sohn, H., & Farrar, C.R. (2001). Vibration-based damage detection using statistical process control. *Mechanical Systems and Signal Processing*, *15*, 707–721.

Ghosh, M., Datta, G.S., Kim, D., & Sweeting, T.J. (2006). Likelihood-based inference for the ratios of regression coefficients in linear models. *Annals of the Institute of Statistical Mathematics*, *58*, 457–473.

Gul, M., & Catbas, F. (2011). Damage assessment with ambient vibration data using a novel time series analysis methodology. *ASCE Journal of Structural Engineering*, *137*, 1518–1526.

Hawkins, D.M., & Zamba, K.D. (2005). Statistical process control for shifts in mean or variance using a change point formulation. *Technometrics*, *47*, 164–173.

He, X., & De Roeck, G. (1997). System identification of mechanical structures by a high-order multivariate autoregressive model. *Computers and Structures*, *64*, 341–351.

Hu, X., Wang, B., & Ji, H. (2013). A wireless sensor network-based structural health monitoring system for highway bridges. *Computer-Aided Civil and Infrastructure Engineering*, *28*, 193–209.

Huang, C.S. (2001). Structural identification from ambient vibration measurement using the multivariate AR model. *Journal of Sound and Vibration*, *241*, 337–359.

Hung, C.F., Ko, W.J., & Peng, Y.T. (2004). Identification of modal parameters from measured input and output data using a vector backward auto-regressive with exogeneous model. *Journal of Sound and Vibration*, *276*, 1043–1063.

Jaishi, B., & Ren, W.X. (2006). Damage detection by finite element model updating using modal flexibility residual. *Journal of Sound and Vibration*, *290*, 369–387.

Jang, S., Spencer, B.F., Rice, J.A., & Wang, J. (2011). Full-scale experimental validation of high fidelity wireless measurement using a historic truss bridge. *Advances in Structural Engineering*, *14*, 93–101.

Kim, C.W., & Kawatani, M. (2008). Pseudo-static approach for damage identification of bridges based on coupling vibration with a moving vehicle. *Structure and Infrastructure Engineering*, *4*, 371–379. doi: 10.1080/15732470701270082

Kiremidjian, A.S., Kiremidjian, G., & Sarabandi, P. (2011). A wireless structural monitoring system with embedded damage algorithms and decision support system. *Structure and Infrastructure Engineering*, *7*, 881–894. doi: 10.1080/15732470903208773

Kumar, R.P., Oshima, T., Mikami, S., Miyamori, Y., & Yamazaki, T. (2012). Damage identification in a lightly reinforced concrete beam based on changes in the power spectral density. *Structure and Infrastructure Engineering*, *8*, 715–727. doi: 10.1080/15732471003730674

Labuz, E.L., Pakzad, S.N., & Wurst, D. (2011). Localized damage detection in a large-scale moment connection using a strain gauge sensor network. In *Proceedings of the SPIE Sensors and Smart Structures Technologies*, San Diego, CA (Vol. 7981, pp. 79813Q-1–79813Q-11). doi: 10.1117/12.880752

Lu, Y., & Gao, F. (2005). A novel time-domain auto-regressive model for structural damage diagnosis. *Journal of Sound and Vibration*, *283*, 1031–1049.

Lynch, J.P., Wang, Y., Loh, K.J., Yi, J.H., & Yun, C.B. (2006). Performance monitoring of the Geumdang bridge using a dense network of high-resolution wireless sensors. *Smart Materials and Structures*, *15*, 1561–1575.

Moaveni, B., Stavridis, A., Lombaert, G., Conte, J.P., & Shing, P.B. (2013). Finite element model updating for assessment of progressive damage in a three-story infilled RC frame. *ASCE Journal of Structural Engineering*, *139*, 1665–1674. doi: 10.1061/(ASCE)ST.1943-541X.0000586

Montgomery, R.H., & Loftis, J.C. (1987). Applicability of the *t*-test for detecting trends in water quality variables. *American Water Resources Association*, *23*, 653–662.

Mosavi, A.A., Dickey, D., Seracino, R., & Rizkalla, S. (2012). Identifying damage locations under ambient vibrations utilizing vector autoregressive models and mahalanobis distances. *Mechanical Systems and Signal Processing*, *26*, 254–267.

Nair, K.K., Kiremidjian, A.S., & Law, K.H. (2006). Time series-based damage detection and localization algorithm with application to the ASCE benchmark structure. *Journal of Sound and Vibration*, *291*, 349–368.

Nigro, M.B., Pakzad, S.N., & Dorvash, S. (2014). Localized structural damage detection: A change point analysis. *Computer-Aided Civil and Infrastructure Engineering*, *29*, 416–432. doi: 10.1111/mice.12059

Noh, H.Y., Nair, K.K., Kiremidjian, A.S., & Loh, C.H. (2009). Application of time series based damage detection algorithms to the benchmark experiment at the National Center for Research on Earthquake Engineering (NCREE) in Taipei, Taiwan. *Smart Structures and Systems*, *5*, 95–117.

Pakzad, S.N. (2010). Development and deployment of large scale wireless sensor network on a long-span bridge. *Smart Structures and Systems*, *6*, 525–543.

Pandey, A.K., & Biswas, M. (1995). Damage diagnosis of truss structures by estimation of flexibility change. *The International Journal of Analytical and Experimental Modal Analysis*, *10*, 104–117.

Srivastava, M.S., & Worsley, K.J. (1986). Likelihood ratio tests for a change in the multivariate normal mean. *Jounral of the American Statistical Association*, *81*, 199–204.

Sohn, H., Farrar, C.R., Hunter, N.F., & Worden, K. (2001). Structural health monitoring using statistical pattern recognition techniques. *ASME Journal of Dynamic Systems, Measurement and Control: Special Issue on Identification of Mechanical Systems*, *123*, 706–711.

Sullivan, J.H., & Woodall, W.H. (1996). A control chart for preliminary analysis of individual observations. *Journal of Quality Technology*, *28*, 265–278.

Weber, B., & Paultre, P. (2010). Damage identification in a truss tower by regularized model updating. *ASCE Journal of Structural Engineering*, *136*, 307–316.

Welch, B.L. (1947). The generalization of 'Student's' problem when several different population variances are involved. *Biometrika*, *34*, 28–35.

West, W.M. (1984). Illustration of the use of modal assurance criterion to detect structural changes in an orbiter test specimen. In *Proceedings of Air Force Conference on Aircraft Structural Integrity* (pp. 1–6).

Wilcox, M. (2003). The philosophy of shewhart's theory of prediction. In *Proceedings of the 9th Research Seminar: Deming Scholar's Program*, New York, USA. Retrieved from http://www.flowmap.com/documents/shewhart.pdf

Yao, R., & Pakzad, S.N. (2012). Autoregressive statistical pattern recognition algorithms for damage detection in civil structures. *Mechanical Systems and Signal Processing*, *31*, 355–368.

Yao, R., & Pakzad, S.N. (2013). Performance comparison of different autoregressive damage features using acceleration measurements from a truss bridge. In *Proceedings of the 9th International Workshop on Structural Health Monitoring*, Stanford, CA (Vol. 1, pp. 220–227).

Zamba, K.D., & Hawkins, D.M. (2006). A multivariate change-point model for statistical process control. *Technometrics*, *48*, 539–549.

Zhang, J., Zou, C., & Wang, Z. (2010). A control chart based on likelihood ratio test for monitoring process mean and variability. *Quality and Reliability Engineering International*, *26*, 63–73.

Zheng, H., & Mita, A. (2007). Two-stage damage diagnosis based on the distance between ARMA models and pre-whitening filters. *Smart Materials and Structures*, *16*, 1829–1836.

Zheng, H., & Mita, A. (2009). Localized damage detection of structures subject to multiple ambient excitations using two distance measures for autoregressive models. *Structural Health Monitoring*, *8*, 207–222.

Zhou, Q., Luo, Y., & Wang, Z. (2010). A control chart based on likelihood ratio test for detecting patterned mean and variance shifts. *Computational Statistics and Data Analysis*, *54*, 1634–1645.

Zou, C., Zhang, Y., & Wang, Z. (2006). A control chart based on a change-point model monitoring linear profiles. *IIE Transactions*, *38*, 1093–1103.